Extended Angular Range of a Three-Hole Cobra Pressure Probe for Incompressible Flow

Argüelles Díaz, K.M.; Fernández Oro, J.M.;
Blanco Marigorta, E.

University of Oviedo, Fluid Mechanics Group.
Campus de Viesques, 33271, Gijón (Asturias), Spain.
arguelleskatia@uniovi.es

ABSTRACT

This paper analyzes the operative characteristics of a three-hole cobra type probe especially designed to attain an angular range higher than 180 deg for planar turbulent flows. A new calibration and data reduction method is also introduced, discriminating three different zones inside the angular range of the calibration. This methodology improves the probe performance, extending its operative angular range from the typical ±30 deg to ±105 deg. In addition, the transmission of the uncertainty – from the pressure measurements to the flow variables – is estimated, showing reasonably low levels for the whole angular range. Furthermore, the sensibility of the probe calibration to the Reynolds number and the pitch angle is considered, and the influence of the turbulence level is outlined. Regarding these factors, the probe precision in the extended angular range is found to be similar to that of the traditional range. Finally, the probe is tested in a flow field with large variations of the incidence angle, and the results obtained with the new method are compared to those given by the traditional calibration.

INTRODUCTION

Pressure and velocity of incompressible flows can be measured in a plane using three-hole pressure (THP) probes. Typically, these probes have angular ranges around ±30 deg, with slight variations depending on the probe type [1].

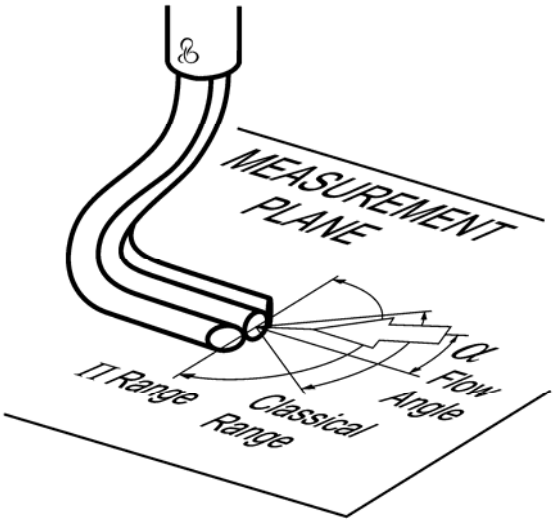

Figure 1. Three-hole cobra type probe.

Recently, some procedures to extend the operative angular range of THP probes have been developed by the authors [2]. In that research, it was suggested that angular ranges higher than 180 deg could be attained using cobra type probes (figure 1), with construction angles between 30 and 40 deg. The present paper describes a calibration and data reduction method employed with a probe of such characteristics, in order to obtain the maximum possible angular range.

The cobra type probe operates with a "non-nulling" mode using a direct calibration method. The "non-nulling" mode keeps the probe position fixed, and uses the pressure measured in the probe holes to obtain the velocity magnitude and the flow direction [3]. This method is less time-consuming that the "nulling" mode because there is no need to orientate the probe during the measurements. Also, using fast-response pressure transducers, it is possible to measure unsteady flows and even turbulence ([4]-[6]). Moreover, the direct calibration procedure has the advantage to take into account the specific effects of the probe geometry [7].

Cobra type probes not only exhibit a higher angular range than cylindrical probes, but also they are unaffected by von Kárman's vortex shedding. However, they are less stable to variations in the Reynolds number than cylindrical geometries.

The maximum attainable angular range is limited by double points and duplicated zones in the data reduction equations. A complete description of this topic can be found in references [2] and

[8]. Double points compromise the unequivocal determination of the flow angle (α), and limit the maximum angular range for probes with construction angles higher than 35 deg. On the other hand, the arising of duplicated zones implies that a single angular interval cannot be directly identified from the pressure measurements. The maximum angular range is limited by the appearance of duplicated zones for probes with construction angles under 35 deg.

Typically, THP probes are designed with a construction angle of 45 deg [9]. In a recent analysis ([2]), it was found that the highest angular range would be reached in the region where double points and duplicated zones boundaries overlap. To corroborate the theoretical analysis, a 35-deg cobra type probe has been built.

This paper analyzes the performance of the probe using a zone-based data reduction method to extend its operative angular range. Also, the uncertainty transmission and other effects that influence the probe accuracy are addressed.

PROBE GEOMETRY

The geometry of the cobra type probe is shown in figure 2. The mechanical design is based on previous experiences in the construction of hot-wire anemometry probes [10].

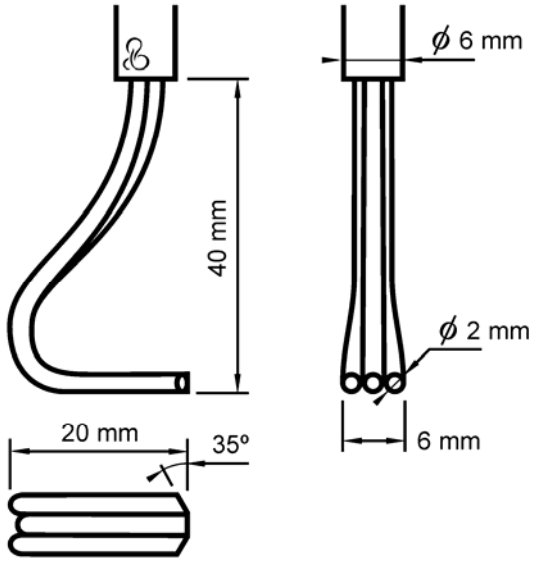

Figure 2. Sketch of the cobra type probe.

The probe is composed of three aluminium tubes, with external and internal diameters of 2 and 1.5 mm. The frontal section of the probe is thus 6 x 2 mm^2. The flow Reynolds number is defined with a characteristic length of 6 mm. The construction angle (35 deg), corresponds to the angle between the faces of the central and each lateral hole. The probe holder, normal to the measurement plane, is 6 mm in diameter.

CALIBRATION METHOD

In a typical calibration procedure, a THP probe is placed on a setup that provides a uniform flow. The probe is axially rotated to change the flow incidence angle [11]. For each position, the pressures in the probe holes (P_1, P_2 and P_3) are stored, together with the position angle (α) and the flow magnitude in the setup. The flow magnitude is usually defined through the static and dynamic pressures (P_s and P_d) at the measurement section with a Pitot-static probe.

The test rig used is a small wind tunnel with an open test section. The probe was positioned from -120 to 120 deg with a step-motor driven support, recording data every 5 deg. The baseline calibration was conducted at 45 m/s, corresponding to a Reynolds number of $1.8 \cdot 10^4$.

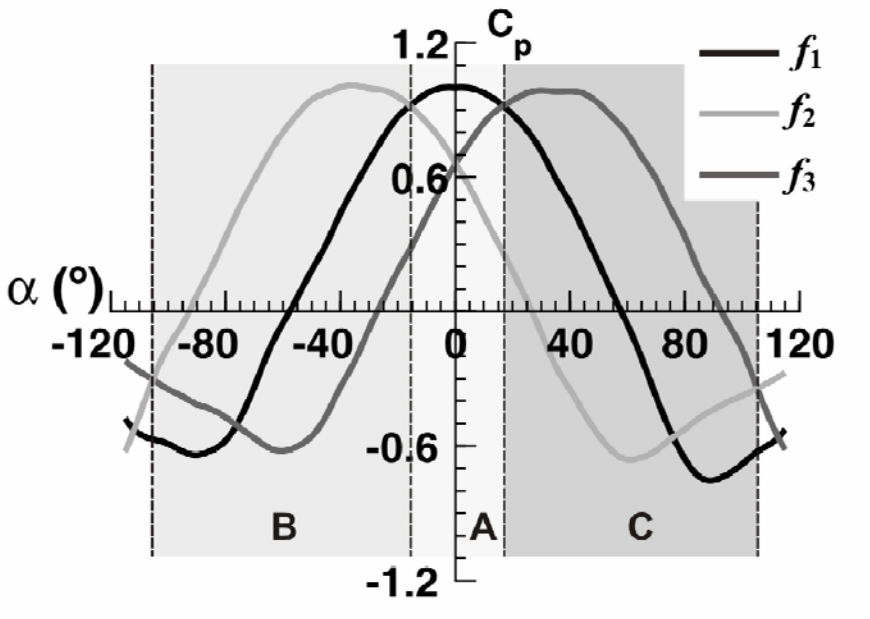

Figure 3. Pressure coefficient distributions in the holes of the cobra type probe.

Figure 3 shows the pressure distributions measured in the holes of the probe, as a function of the flow angle. They have been normalized as typical pressure coefficients: $f_i = (P_i - P_s)/P_d$. Maximum values (f_i = 1) are obtained for relative zero-incidence flow angles in each hole: 0 deg for the central and +35 and -35 deg for the right and left holes respectively. Minimum values are found when the flow is aligned with the face of the holes: ±90 deg for the central one ($f_1 \approx$ -0.8) and +55 and -55 deg for left and right holes respectively.

The traditional calibration method defines normalized coefficients (angular coefficient C_α, total pressure coefficient C_{Po}, and static pressure coefficient C_{Ps}), relating the values registered during the calibration [12]:

$$C_\alpha = \frac{P_2 - P_3}{P_1 - 0.5(P_2 + P_3)}$$
$$C_{P_0} = \frac{P_0 - P_1}{P_1 - 0.5(P_2 + P_3)} \qquad (1)$$
$$C_{P_s} = \frac{P_0 - P_s}{P_1 - 0.5(P_2 + P_3)}$$

where P_0 and P_s represent the total and static pressures in the setup, and P_1, P_2 and P_3 correspond to the pressures in the central, left and right holes of the probe respectively. With the value of these coefficients in each angular position, the calibration curves of the probe are constructed. Once the calibration is completed, those curves are employed to retrieve the direction and velocity magnitude of the measured flow [13], according to the procedure shown in figure 4. In this data reduction procedure the value of C_α is obtained for each measurement with the pressures recorded in the three holes, using the first expression in (1). From the C_α calibration curve, the flow angle α is determined (upper graphic in figure 4). Once α is known, the values of C_{Po} and C_{Ps} for that particular angle are obtained from their own calibration curves (bottom graphic). Then, P_0 and P_s are calculated with the second and third expressions in (1). Finally, the difference between them, i.e. the dynamic pressure, provides the velocity magnitude of the flow.

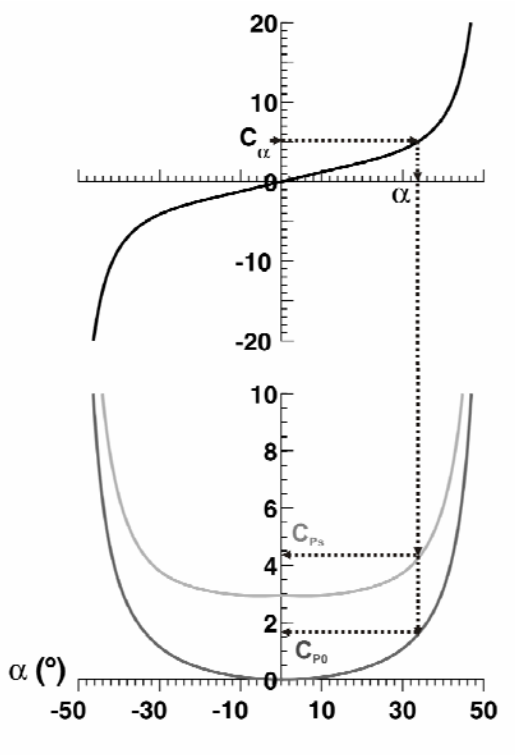

Figure 4. Traditional calibration coefficients and data reduction procedure.

With the traditional calibration, the operative angular range of the probe is about ±48 deg, due to the presence of singular points at -50 and +50 deg in the angular coefficient.

To avoid these singularities, a zone-based data reduction method has been defined. This method discriminates three different zones for the angular range of the calibration, which are identified using the pressures measured in the holes. In particular, each zone corresponds to the angular interval where one of the pressures in the holes is higher than the others. Figure 3 shows these three zones: A when P_1 is the highest pressure, B and C when P_2 and P_3 are the highest values respectively. For each zone a different angular coefficient is established:

$$C_\alpha = \frac{P_2 - P_3}{P_1 - 0.5\left(P_2 + P_3\right)} \quad \text{zone A} \tag{2}$$

$$C_\alpha = \frac{P_3 - P_2}{P_2 - 0.5\left(P_1 + P_3\right)} + 4 \quad \text{zone B} \tag{3}$$

$$C_\alpha = \frac{P_3 - P_2}{P_3 - 0.5\left(P_1 + P_2\right)} - 4 \quad \text{zone C} \tag{4}$$

Accordingly, both total and static pressure coefficients are also defined:

$$C_{P_0} = \frac{P_0 - P_1}{P_1 - 0.5\left(P_2 + P_3\right)} \quad \text{zone A} \tag{5}$$

$$C_{P_0} = \frac{P_0 - P_1}{P_2 - 0.5\left(P_1 + P_3\right)} \quad \text{zone B} \tag{6}$$

$$C_{P_0} = \frac{P_0 - P_1}{P_3 - 0.5\left(P_1 + P_2\right)} \quad \text{zone C} \tag{7}$$

$$C_{P_s} = \frac{P_0 - P_s}{P_1 - 0.5\left(P_2 + P_3\right)} \quad \text{zone A} \tag{8}$$

$$C_{P_s} = \frac{P_0 - P_s}{P_2 - 0.5\left(P_1 + P_3\right)} \quad \text{zone B} \tag{9}$$

$$C_{P_s} = \frac{P_0 - P_s}{P_3 - 0.5\left(P_1 + P_2\right)} \quad \text{zone C} \tag{10}$$

The angular coefficients (2)-(4) have no singular points in the zones where each one is defined. In addition, they are monotonous functions with the flow angle, allowing an extension of the operative angular range. Other expressions for the angular coefficient could be chosen [2], but the relations previously introduced have been selected because the similarity to the traditional coefficients. Specifically, the +4 and -4 values in equations (3)-(4) have been added to obtain a continuous function of the angular coefficient throughout the three zones, simplifying its graphic representation and the flow field determination.

Figure 5 compares the angular coefficient defined through (2)-(4) (solid line) with the traditional one (dashed line). Obviously, both coefficients are equal in zone A. It can be observed that, using the traditional calibration, this cobra type probe provides an important angular range (±48 deg), notably higher than typical ranges (±30 deg) found in the literature for THP probes. However, with the zone-based data reduction method, the angular range is extended up to ±105 deg. In this case, the limit is due to the appearance of duplicated zones, and not to the arising of double points: for instance, when the flow angle is higher than 105 deg, $P_2 > P_1 > P_3$, which is the same

condition already fulfilled in zone B. As a result, this external zone cannot be distinguished from previous zone B and thus the angular range has to be limited to ±105 deg.

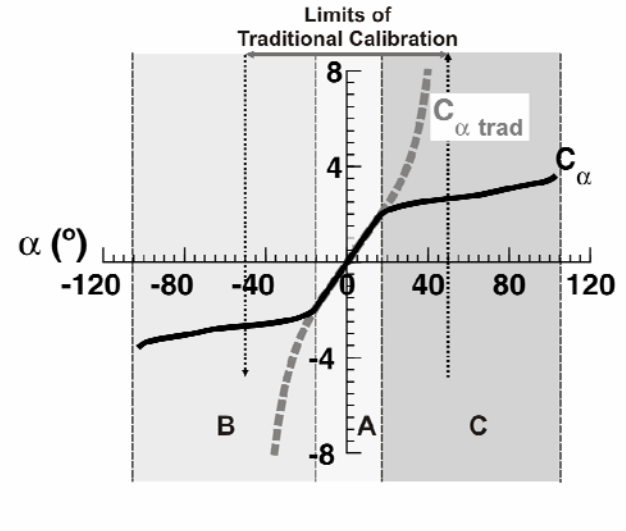

Figure 5. Angular calibration coefficient: zone-based (solid) and traditional methods (dashed line).

UNCERTAINTY TRANSMISSION

In this section, the uncertainty transmitted from the pressures measured in the holes of the cobra type probe to the flow variables is estimated. This uncertainty is calculated based on the method proposed by Kline [14] (further details can be found in [2]):

$$I_\alpha = \frac{I_p}{P_d} \cdot \frac{\sqrt{(f_3 - f_2)^2 + (f_1 - f_3)^2 + (f_2 - f_1)^2}}{f_1'(f_3 - f_2) + f_2'(f_1 - f_3) + f_3'(f_2 - f_1)} \tag{11}$$

$$I_{Pd} = I_p \cdot \frac{\sqrt{\left(f_3' - f_2'\right)^2 + \left(f_1' - f_3'\right)^2 + \left(f_2' - f_1'\right)^2}}{f_1'(f_3 - f_2) + f_2'(f_1 - f_3) + f_3'(f_2 - f_1)} \tag{12}$$

$$I_{Ps} = I_p \cdot \frac{\sqrt{\left(f_2 f_3' - f_3 f_2'\right)^2 + \left(f_3 f_1' - f_1 f_3'\right)^2 + \left(f_1 f_2' - f_2 f_1'\right)^2}}{f_1'(f_3 - f_2) + f_2'(f_1 - f_3) + f_3'(f_2 - f_1)} \tag{13}$$

In these expressions, I_α denotes the uncertainty of the flow angle, while I_{Pd} and I_{Ps} are the uncertainty of the dynamic and static pressures respectively. I_p is the uncertainty of the pressure

measured by the transducers, which is supposed to be the same for the three holes of the probe. $f_i'(i = 1,2,3)$ are the derivatives of the pressure coefficients f_i with respect to the flow angle. Equations (11)-(13) show that the uncertainty transmission to the final results depends only on the pressure coefficient distributions. Furthermore, it has been found that the uncertainty, although different for each specific geometry, is independent of the data reduction procedure employed.

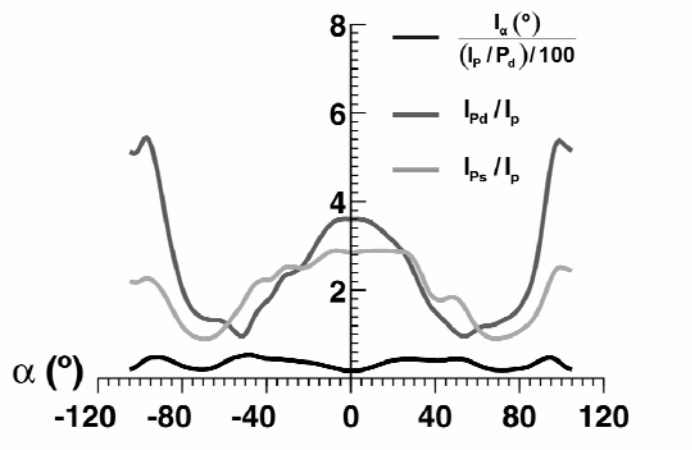

Figure 6. Uncertainty of the flow variables.

Figure 6 shows the uncertainty results for this cobra type probe, estimated from expressions (11)-(13) with the pressure coefficients shown in figure 3. It represents the angle uncertainty (black line), and the uncertainties of the dynamic (dark gray line) and static (light gray line) pressures. The uncertainty of the flow angle is expressed as a percentage of the uncertainty in the pressure measurement, I_p, relative to the dynamic pressure, P_d. Both dynamic and static pressure uncertainties are referenced to the uncertainty in the pressure measurement, I_p. These latter uncertainties are from two to four times higher than in the case of cylindrical probes [2]. However, since the pressure uncertainty of typical transducers is quite low (from 0.1% to 0.25% of the nominal range), the absolute uncertainty levels are reasonably small. Moreover, the uncertainty distributions shown in figure 6 are the same than those of the traditional calibration in the common angular interval.

The angle uncertainty does not exceed 0.6 deg for every 1% of I_p/P_d in the whole angular range. In the case of zero-incidence flows, this uncertainty is barely 0.2 deg for every 1% of I_p/P_d.

Also, the uncertainty levels for both dynamic and static pressures are respectively 3.6 and 2.8 times I_p. The dynamic pressure uncertainty reaches the maximum values around ±95 deg, while the minimum values are found at ±50 deg. The static pressure uncertainty has its maximum at zero-incidence flow, with the minimum values around ±70 deg, which are progressively increased towards the limits of the operating range.

REYNOLDS NUMBER EFFECTS

Previous sections described a zone-based procedure to improve the angular range of a cobra type probe. Also, the uncertainty transmission from the measurements to the results has been analyzed to characterize the probe accuracy. However, the major source of error for THP probes derives from the difference between the velocity adopted in the calibration and the measured velocity.

The analysis of the previous sections was conducted assuming that the pressure coefficient distributions are independent of the velocity magnitude, i.e., they are exclusively a function of the incidence angle α. Nevertheless, this is true only for a certain Reynolds number range, which even depends on the particular geometry of the probes. To outline the sensibility of the probe calibration to Reynolds number variations, different flow velocities were tested to obtain the pressure coefficients.

In the calibration setup, yaw angles ranging from -120 to 120 deg were considered every 5 deg. The measurements were obtained for five different velocities, from 25 to 65 m/s, corresponding to Reynolds numbers from $1.0 \cdot 10^4$ to $2.6 \cdot 10^4$. Figure 7 shows the pressure coefficient distributions measured for the five Reynolds numbers. The figure includes all the angular coefficient distributions obtained with the zone-based method. The effect of the flow velocity is practically negligible for yaw angles within ±70 deg. The most significant variations are observed in the central hole pressure coefficient, when the yaw angle is beyond ±75 deg. For these external

zones, the f_1 values decrease as the Reynolds number increases, with maximum variations around ±90 deg.

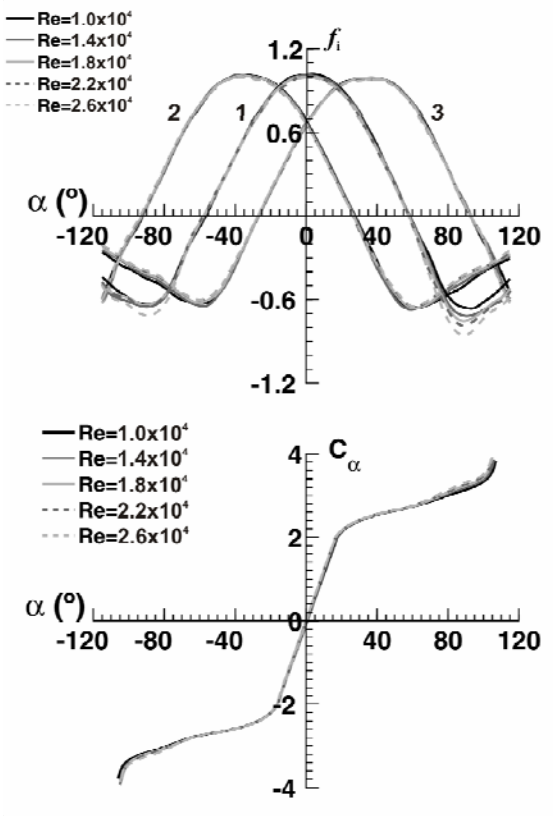

Figure 7. Pressure and angular coefficients for different flow Reynolds numbers.

Data corresponding to Reynolds numbers of $1.0 \cdot 10^4$, $1.4 \cdot 10^4$, $2.2 \cdot 10^4$ and $2.6 \cdot 10^4$, were reduced with the zone-based method using the calibration of an intermediate Reynolds ($1.8 \cdot 10^4$). The results have been compared with the real values to estimate the error introduced. Figure 8 represents the absolute error in the determination of the angle (Err) as a function of the real flow angle (α). As expected, the error increases with the difference between calibration and measured velocities. For centered intervals, ±40 deg, the error is less than 1 deg. It maintains reasonably low values (under 2.5 deg) from ±40 to ±75 deg; but it increases severely beyond that limit (where the largest variations of the pressure coefficients were observed in figure 7).

It is a good practice to complete several calibrations for different Reynolds numbers when there is a large variation in the velocity magnitude (or a high precision is required). Figure 8 shows a progressive enlargement of the errors, increasing with the deviation in the velocity magnitude

from the baseline calibration. Assuming a linear dependence between them (at least in averaged terms), an alternative methodology has been introduced, interpolating different calibrations in order to obtain more accuracy in the flow variables.

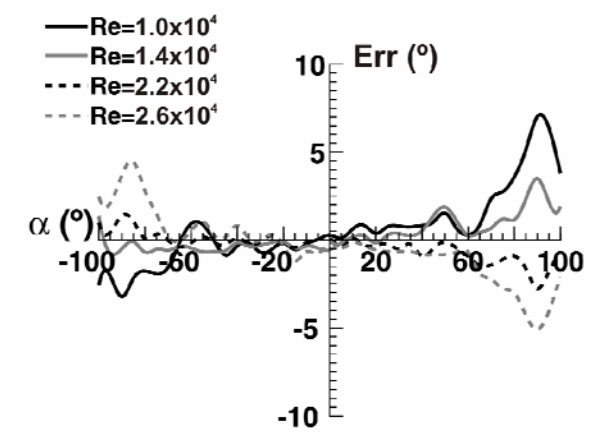

Figure 8. Errors in the estimation of the flow angle using a reference calibration of Re = $1.8 \cdot 10^4$.

The results of this procedure are illustrated in figure 9. It shows the errors when the data reduction is done interpolating between calibrations at extreme Reynolds numbers: $1.0 \cdot 10^4$ and $2.6 \cdot 10^4$. In the ±45 deg interval, the error is now reduced to values under 0.6 deg. External ranges present higher values, but not exceeding 2 deg of absolute error. Moreover, the maximum relative error introduced for the determination of the velocity magnitude is 5%, with a 4% error in the static pressure measurement.

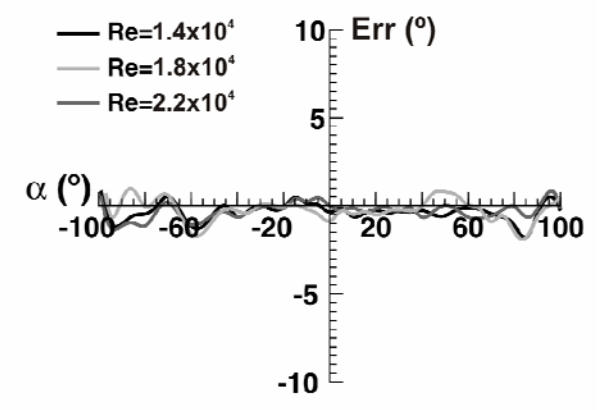

Figure 9. Errors in the estimation of the flow angle when interpolating between two calibrations at different Reynolds numbers.

PITCH ANGLE AND TURBULENCE LEVEL EFFECTS

Another error is caused by the deviation of the flow from the probe measurement plane. It is considered that THP probes provide accurate results if the pitch angle β (angle between the flow and the probe measurement plane) does not exceed 10 or 12 degrees (cfr. [1] and [12]). In addition, it is to be expected that the pitch angle influence increases with the yaw angle. Then, its effect would be more evident in the extended range of the zone-based method.

A set of tests has been carried out to characterize this influence. The angular coefficient has been obtained for the whole calibration range varying the pitch angle from 0 to 20 deg every 2.5 deg. All the test were conducted for the baseline Reynolds number of $1.8 \cdot 10^4$.

Figure 10 shows these angular coefficients. Due to the symmetry of the results, only positive values of the yaw angle have been plotted. From 0 to 60 deg, the angular coefficients reveal only small differences even for pitch angles as high as 20 deg. From 60 deg on, the difference becomes more evident, increasing with both pitch and yaw angles.

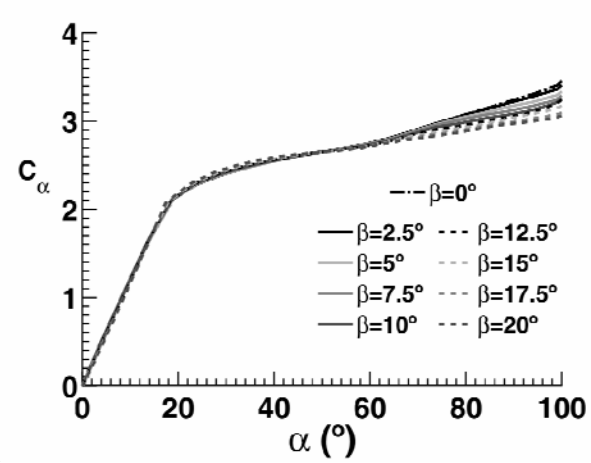

Figure 10. Influence of the pitch angle β on the angular coefficient.

In order to quantify the effect of the pitch angle, these measurements have been used to determine the error introduced when the zero pitch calibration is employed with flows of non-zero pitch angle. Figure 11 shows, for each pitch series, the difference between the yaw angle obtained using the zone-based method and the real yaw angle set in the calibration setup. This allows a better appreciation of the pitch angle influence.

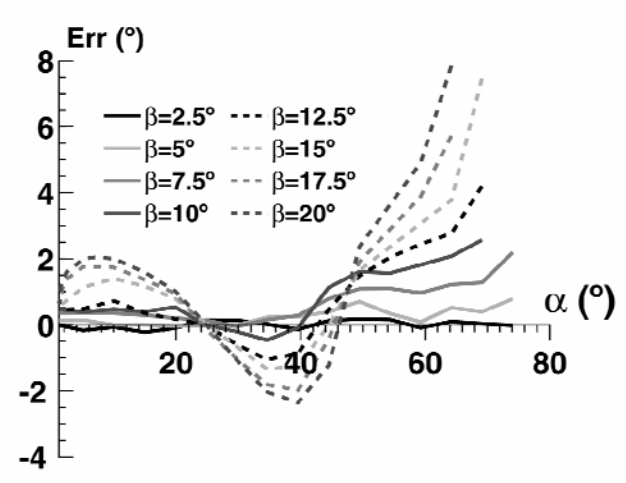

Figure 11. Errors in the yaw angle determination with different pitch angles.

For yaw angles between 0 and 45 deg, the error remains below 1 deg if the pitch angle is smaller than 10 deg. For yaw angles above 45 deg, the pitch angle should be kept below 5 deg to obtain the same accuracy. Pitch angles above 15 deg give too much error even for low yaw angles, although up to 50 deg the error remains below 3 deg for β as high as 20 deg.

The effect of the turbulence level is also closely related to the pitch angle influence. Cobra type probes are less sensitive to turbulence than the three-hole cylindrical probes, because they develop bluff-body separations instead of a boundary-layer detachment over a convex surface. Nevertheless, there are two effects of the turbulence level over the probe accuracy: the error induced over the pressure value and the flow angle deviation (cfr. [9] and [15]). The first effect is considered low if the turbulence intensity is not too high; Chue [15] reports a total pressure change of only 2% with a turbulence intensity of 20%. Also, this effect can be taken into account using fast-response transducers (a correction of the line-cavity system can be needed [4]-[6]). On the other hand, the flow angle deviation can only be partially determined with fast-response transducers because fluctuations occur in both yaw and pitch angles.

No specific tests have been carried out to analyze the influence of the turbulence level on this cobra type probe. However, concerning the deviation of the flow angle, a relation could be assumed between the turbulence intensity and a certain amplitude of angular oscillations. In particular, Walsche et al. [16] argue that 15 deg correspond to a quite strong intensity: about 40%. Therefore, it

is expected for the probe to be rather insensitive to turbulence in the range of the traditional calibration: an amplitude of 10 deg been analogous to a turbulence level around 25%. On the other hand, if a good accuracy has to be maintained for the whole extended angular range, the turbulence level of the flow should be lower (an amplitude of 5 deg, about 10%…).

MEASUREMENT TEST

The performance of the cobra type probe has been tested in a flow field with large variations in the incidence angle.

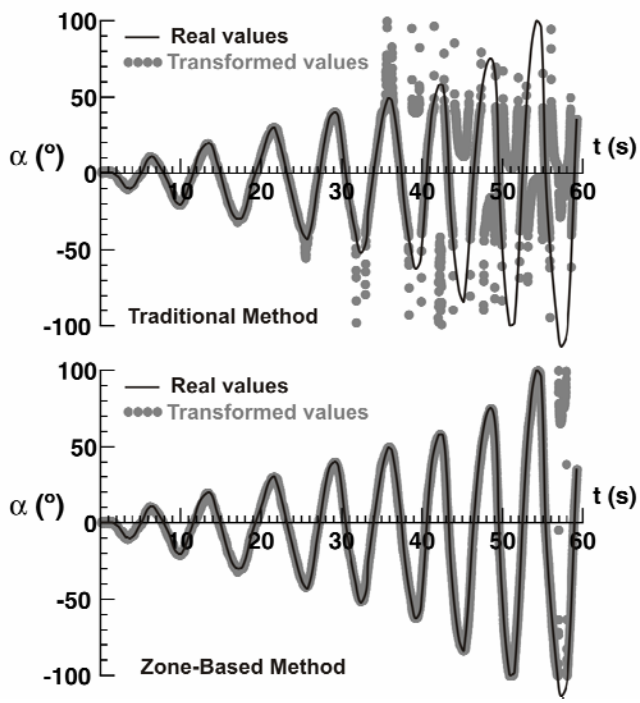

Figure 12. Flow angle measurements obtained with the traditional calibration and with the zone-based data reduction method.

The probe was mounted in the calibration setup on a support able to generate an oscillating angular motion. The flow velocity, maintained constant, was measured with a Pitot-static probe. The angular oscillation was continuously measured using a goniometer of 0.25 deg precision. The amplitude of the oscillations was progressively increased from 0 to ±120 deg. The pressure values of the probe holes were acquired with a frequency of 100 Hz during 60 seconds, together with the

angular position and the flow velocity. The flow variables were calculated using both traditional and zone-based data reduction methods.

The retrieved flow angles are shown in figure 12, compared to the real values. Fluctuations in the flow direction within ±40 deg are accurately described by both methods. When the variations are beyond those angles, the traditional calibration fails, providing an incorrect value of the flow angle. On the contrary, the zone-based method measures correctly variations of the flow angle up to ±100 deg. Beyond this limit, erratic values are also obtained.

CONCLUSIONS

A three-hole cobra type probe with a construction angle of 35 deg has been designed and built to measure flow fields with strong variations of the incidence angle.

A zone-based method has been defined for the data reduction procedure, extending the operative angular range from the ±48 deg of the traditional calibration to ±105 deg. The uncertainty transmission has been analyzed and the values in the extended angular range have been found to be similar to those in the traditional range.

The effect of the Reynolds number on the probe performance has also been studied. A methodology, based on the interpolation between two calibrations for different Reynolds numbers, was proposed. It has been shown that this strategy reduces the errors even in the extended angular range, to 2 deg in the angle, 5% in the velocity magnitude and 4% in the static pressure.

In addition, the influence of pitch angle deviations has been tested. The results show that pitch angles below 10 deg are acceptable in the traditional range, while 5 deg is the maximum admissible deviation to obtain the same accuracy in the extended range.

Finally, a measurement test was conducted in a flow with large variations in the incidence angle. It is shown that the traditional calibration provides accurate results up to ±40 deg, while the zone-based method enlarges the attainable span more than two times, reaching up to ±100 deg.

ACKNOWLEDGEMENTS

This work was supported by the Research Project "Effect of the volute geometry of centrifugal pumps on the fluid-dynamic perturbations due to rotor-stator interaction", ref. DPI-2006-15638-C02-01, MEC.

NOMENCLATURE

THP	Three-Hole Probe
C_α	Angular coefficient
C_{Po}	Total pressure coefficient
C_{Ps}	Static pressure coefficient
Err	Absolute error, [deg]
f_i	Pressure coefficient, i = 1,2,3
I_α	Angle uncertainty, [deg]
I_P	Pressure uncertainty, [Pa]
I_{Pd}	Dynamic pressure uncertainty, [Pa]
I_{Ps}	Static pressure uncertainty, [Pa]
P_1	Central hole pressure measurement, [Pa]
P_2	Left hole pressure measurement, [Pa]
P_3	Right hole pressure measurement, [Pa]
P_d	Dynamic pressure, [Pa]
P_0	Total pressure, [Pa]
P_s	Static pressure, [Pa]
Re	Reynolds number
t	Time, [s]

Greek letters

α	Flow angle (yaw angle), [deg]

β	Pitch angle, [deg]
δ	Construction angle of the probe, [deg]

REFERENCES

[1] Dudziniski T J, Krause L N 1969 Flow-direction measurement with fixed-position probes *NASA TM X-1904*

[2] Argüelles Díaz K M, Fernández Oro J M, Blanco Marigorta E 2008 Direct calibration framework of triple-hole pressure probes for incompressible flow *Measurement Science and Technology* **19** 075401 (13pp)

[3] Wuest W 1967 Measurement of flow speed and flow direction by aerodynamic probes and vanes *AGARD Conference Proceedings* **32** 373-426

[4] Hooper J D, Musgrove A R 1997 Reynolds stress, mean velocity, and dynamic and static pressure measurement by a four-hole pressure probe *Experimental Thermal and Fluid Science* **15** 375-383

[5] Guo Y, Wood D H 2001 Instantaneous velocity and pressure measurements in turbulent mixing layers *Experimental Thermal and Fluid Science* **24** 139-150

[6] Chen J, Haynes B S, Fletcher D F 2000 Cobra probe measurements of mean velocities, Reynolds stresses and higher-order velocity correlations in pipe flow *Experimental Thermal and Fluid Science* **21** 206-217

[7] Treaster A L, Yocum A M 1979 The calibration and application of five-hole probes *ISA Transactions* **18** 23-34

[8] Argüelles Díaz K M, Fernández Oro J M, Blanco Marigorta E 2008 Three-hole pressure probes at large *Proceedings of XIXth Symposium on Measuring Techniques for Transonic and Supersonic Flows in Cascades and Turbomachines* Belgium

[9] Tropea C, Yarin A L, Foss J F (Eds) 2007 Springer handbook of experimental fluid mechanics *Springer.Verlag ISBN: 978-3-540-25141-5*

[10] Blanco E, Ballesteros R, Santolaria C 1998 Angular range and uncertainty analysis of non-orthogonal crossed hot wire probes *Journal of Fluids Engineering* **120** 90-94

[11] Lewis W E 1966 Fixed-direction probes for aerodynamic measurements *Proc. Inst. Mech. Eng.* **180** 141-152

[12] Bryer D W, Pankhurst R C 1971 Pressure-probe methods for determining wind speed and flow direction *National Physical Laboratory ISBN: 011-480012X*

[13] Sumner D 2002 A comparison of data-reduction methods for a seven-hole probe *Journal of Fluids Engineering* **124** 523-527

[14] Kline S J, McClintock F A 1953 Describing uncertainties in single sample experiments *Mechanical Engineering* 3-8

[15] Chue S H 1975 Pressure probes for fluid measurement *Progress in Aerospace Sciences* **16(2)** 147-223

[16] Walsche D E, Garner H C 1960 Usefulness of various pressure probes in fluctuating low speed flows *Brit. ARC 21714*

LIST OF FIGURES

Figure 10. Influence of the pitch angle β on the angular coefficient.

Figure 11. Errors in the yaw angle determination with different pitch angles.

Figure 12. Flow angle measurements obtained with the traditional calibration and with the zone-based data reduction method.